Impact of barrier layer on winter-spring variability of the southeastern Arabian Sea

S. Masson,[1] J.-J. Luo,[1] G. Madec,[2] J. Vialard,[2] F. Durand,[3] S. Gualdi,[4] E. Guilyardi,[5,6] S. Behera,[1] P. Delecluse,[5] A. Navarra,[4] and T. Yamagata[1,7]

Received 12 November 2004; accepted 1 March 2005; published 6 April 2005.

[1] In the present study, we use a coupled model to evaluate the effect of shallow salinity stratification on the sea surface temperature (SST) and on the monsoon onset in the southeastern Arabian Sea (SEAS). A 100-year control experiment shows that the coupled model reproduces the main climatic features in this region in terms of SST, precipitation and barrier layer (BL). A 100-year sensitivity experiment (where BL effects have been suppressed in the SEAS) shows that BL enhances the spring SST warming by 0.5°C, and leads to a statistically significant increase of precipitation in May (3 mm/day) linked to an early (10 to 15 days) monsoon onset. This suggests that the BL extent may be a useful predictor of the summer monsoon onset in the area with a two-month lead-time. However the effect above is mostly concentrated in the SEAS, and there is no significant impact over continental India. **Citation:** Masson, S., et al. (2005), Impact of barrier layer on winter-spring variability of the southeastern Arabian Sea, *Geophys. Res. Lett.*, *32*, L07703, doi:10.1029/2004GL021980.

1. Introduction

[2] From February to May, before the summer monsoon, the temperature in the southeastern Arabian Sea (SEAS, defined by *Durand et al.* [2004] as the 68°E–77°E; 6°N–15°N region) warms up to temperatures exceeding 30°C (Figure 1b). This warming leads to the formation of the so called mini-warm pool [*Sengupta et al.*, 2002]. The seasonal northward migration of the maximum solar radiation, the clear sky and light wind conditions in spring give a basic explanation of this SST warming. However, as underlined by *Shenoi et al.* [1999], the physics of the ocean mixed layer must be involved to explain why the SST in the Lakshadweep Sea increases more rapidly and reaches higher values than it does elsewhere in the Arabian Sea. First, from December to March a large oceanic anticyclonic circulation is observed off the southwestern coast of India. It is associated with a high in the sea level known as the Lakshadweep High (LH) [*Bruce et al.*, 1994; *Shankar and Shetye*, 1997; *Bruce et al.*, 1998]. The LH is mainly produced by downwelling Rossby waves radiated from coastal Kelvin waves propagating poleward along the western coast of India. This feature deepens the thermocline in January–February creating favorable condition for a SST warming in the SEAS. Second, the Winter Monsoon Current brings fresh water coming from the Bay of Bengal into the SEAS [*Shetye et al.*, 1991; *Rao and Sivakumar*, 2003]. This produces a shallow salinity and density stratification which limits the mixed layer depth and creates a thick Barrier Layer (BL) [*Lukas and Lindstrom*, 1991] (Figure 1a) that could explain the large SST warming in the SEAS prior to monsoon onset [*Rao and Shivakumar*, 1999; *Shenoi et al.*, 1999; *Durand et al.*, 2004].

[3] Several studies based on observations [*Rao and Shivakumar*, 1999; *Shenoi et al.*, 1999] suggested that the mini-warm pool influences the onset of the summer monsoon in the eastern Arabian Sea (Figure 1c). *Rao and Shivakumar* [1999] showed that onset of atmospheric vortices [*Krishnamurti et al.*, 1981] formed over the mini-warm pool are mainly associated with early onset of the Indian summer monsoon. The precursor modeling study of *Kershaw* [1985] supported this hypothesis for one particular event but until now, the real impact of the mini-warm pool on the onset of the summer monsoon in the Arabian Sea has not been quantified. Additional work is also needed to confirm and quantify the air-sea interactions that could link the BL to the spring SST warming and then to the summer monsoon precipitation in the SEAS.

[4] In this paper, we propose to explore these remaining questions by using a coupled general circulation model. The next section will briefly describe this model. The results of the coupled model regarding the SST, the precipitation and BL in the SEAS will be discussed and validated in section 3. By using a sensitivity experiment, we explore and quantify the impact of the BL on the SST warming and on the monsoon onset in section 4 before concluding in section 5.

2. Model Presentation

[5] The coupled ocean atmosphere model is the Scale Interaction Experiment-FRCGC (SINTEX-F1) model [*Luo et al.*, 2003] which has been developed from the original European SINTEX model [*Gualdi et al.*, 2003a; *Guilyardi et al.*, 2003]. The ocean component is OPA 8.2 [*Madec et al.*, 1999] with the ORCA2 configuration: $2° \times 2°$ cos(latitude) with increased meridional resolutions to 0.5° near the equator. It has 31 vertical levels with 14 lying in the top 150

[1]Frontier Research Center for Global Change (JAMSTEC), Yokohama, Japan.
[2]Laboratoire d'Océanographie Dynamique et de Climatologie (CNRS/UPMC/IRD), Paris, France.
[3]Laboratoire d'Etudes en Geophysique et Oceanographie Spatiales (CNRS/CNES/UPS/IRD), Toulouse, France.
[4]National Institute of Geophysics and Volcanology, Bologna, Italy.
[5]Laboratoire des Sciences du Climat et l'Environnement (CEA/CNRS), Gif-sur-yvette, France.
[6]Also at NCAS Centre for Global Atmospheric Modeling, University of Reading, UK.
[7]Also at Department of Earth and Planetary Science, Graduate School of Science, University of Tokyo, Tokyo, Japan.

0094-8276/05/2004GL021980

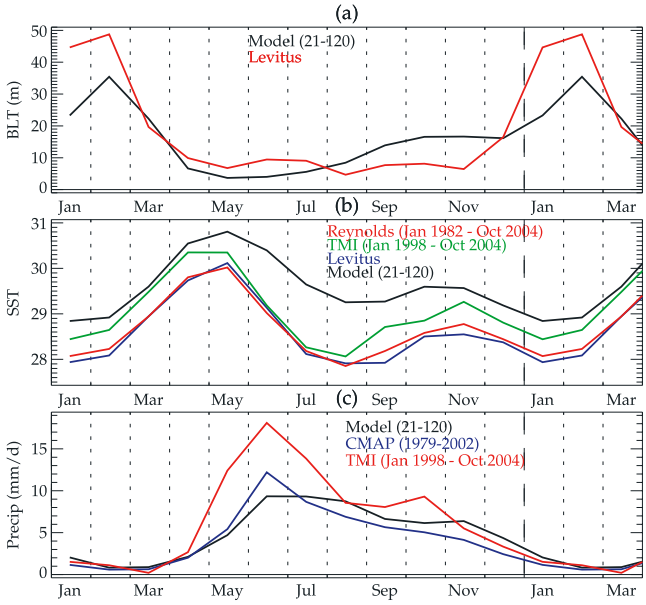

Figure 1. Times series of monthly climatologies over the SEAS domain (68°E–77°E; 6°N–15°N). a: BL thickness (m), b: SST (°C), c: precipitation (mm/day).

meters. The turbulent kinetic energy (TKE) determines the vertical mixing. The atmospheric component is ECHAM4 [*Roeckner*, 1996] with a T106 horizontal resolution and 19 hybrid sigma-pressure levels. A mass flux scheme [*Tiedtke*, 1989] is applied for cumulus convection with modifications for penetrative convection according to *Nordeng* [1994]. The coupling information, without flux correction, is exchanged every two hours by means of the OASIS 2.4 coupler [*Valcke et al.*, 2000]. The BL is computed according to *Sprintall and Tomczak* [1992] criterion.

[6] The reference experiment (REF) was run for 120 years but we keep only the last 100 years as the model reaches its own climatology within the first 20 years. Starting from year 21, we also ran a 100-year sensitivity experiment (PERTURB) in which we suppressed, only in the SEAS, the impact of the salinity stratification on the vertical mixing, as done by *Vialard and Delecluse* [1998]. Note that the salinity is still taken into account in the pressure gradient, even within the SEAS.

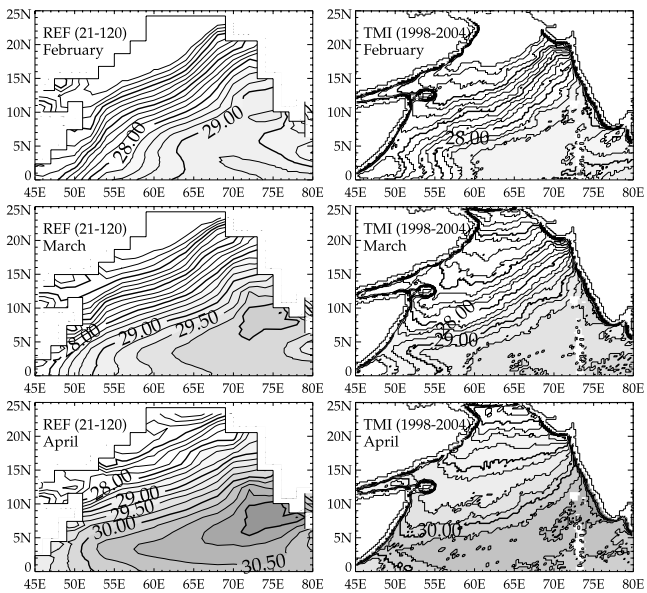

Figure 2. SST (°C) maps for Model (left) and TMI (right) climatologies from February (top) to April (bottom). CI = 0.25°C, thick line every 1°C.

3. Model Results

3.1. SST

[7] Observed SST climatologies show significant differences in the SEAS. The Tropical Rainfall Measuring Mission (TRMM) Microwave Imager (TMI) data is often at least 0.5°C warmer than the other observed data (Figure 1b). Note that exclusion of the warm winter of 1998 from the TMI climatology gives similar results. The excellent quality of TMI that can "see through the clouds" [*Sengupta and Ravichandran*, 2001; *Duvel et al.*, 2004] drives us to select this product for the SEAS which is often covered by clouds during SST warming periods.

[8] Both, model and observation show the warming of the Arabian Sea from February to May with a northwestward propagation of a sharp SST front described by *Durand et al.* [2004] (Figure 2). The mini-warm pool in the SEAS peaks in April–May. The model shows a warm bias: though it is close to TMI in March–April, model SST maximum reaches 30.8°C i.e. higher than TMI (30.4°C), the warmest observed SST climatology. Nevertheless, the 2°C SST warming from January to May fits all observed trends. The underestimation of the model SST cooling in summer is explained by weaker southwesterlies, which are too light to cool the SST as in observation [*Vinayachandran*, 2004].

3.2. Precipitation

[9] Figures 1c and 3 illustrate the differences between precipitation climatologies and the difficulty to make a quantitative validation. The strong variability of TMI precipitation may look suspicious but *Bowman et al.* [2003] showed that TMI has near-zero bias in the Pacific Ocean when compared with the rain gauges.

[10] The model precipitation in the Arabian Sea is realistic with respect to the observed climatologies differences. The coupled model reproduces the location and timing of the monsoon onset (Figure 3). Model time series over the SEAS have amplitude close to CMAP with precipitation

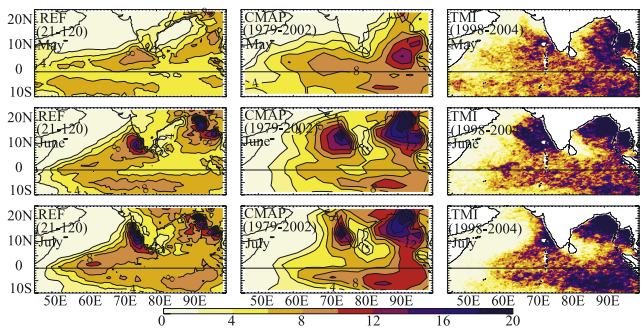

Figure 3. Precipitation (mm/day) maps for Model (left) CMAP (middle) and TMI (right) climatologies from February (top) to April (bottom). CI = 0.25.

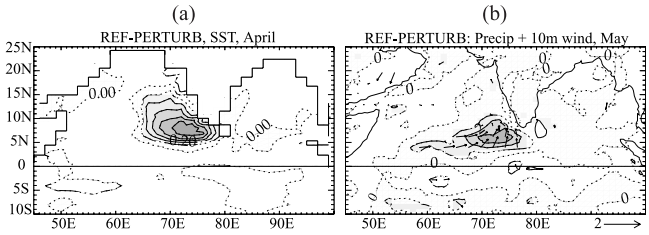

Figure 4. Maps of monthly climatological differences (REF)-(PERTURB). a: SST (°C) in April, CI = 0.1°C. b: 10 m wind (m/s) and Precipitation (mm/day) in May, CI = 1 mm/day, significant areas (95% using a Student's T-test) have solid contours and are shaded.

increasing from April to June (Figure 1c). The decrease in July–August is weakly represented because of the too warm SST at this time (see previous section). In June, large amplitude differences are seen between TMI and CMAP data making the validation difficult. But it is apparent that model precipitation in the Arabian Sea is too much confined along the western coast of India and does not extent enough westward toward the Arabian Sea and eastward over India as suggested by CMAP. Part of this bias is explained by the impossibility to have an accurate representation of the mountain ridge along the western coast of India with the actual atmospheric grid horizontal and vertical resolution.

3.3. Salinity and Barrier Layer

[11] The BL variability in the SEAS has already been documented in a large number of studies [*Rao and Shivakumar*, 1999, 2003; *Shenoi et al.*, 2004; *Durand et al.*, 2004; *De Boyer Montegut et al.*, 2004]. In agreement with the observations, the model BL peaks in January–February with a mean thickness over the SEAS of 30 m (Figure 1a). In agreement with the observations, formation of model BL results mainly from the combination of two mechanisms: the downwelling associated with the LH and the simultaneous input of fresh surface water originating from the Bay of Bengal. The downwelling peaks in February when the top of the thermocline deepens down to 90 m. The input of fresh water raises the pycnocline from 55 m in January to 30 m at the end of March. However, the model underestimates the freshening trend of the surface layer and its sea surface salinity (SSS) remains larger than 34.7 psu whereas Levitus climatology and other observations [*Rao and Sivakumar*, 2003; *Delcroix et al.*, 2005] suggest that SSS in the SEAS drops between 34 and 34.5 psu in January. This model deficiency, originating mostly from a SSS bias in the Bay if Bengal, limits the shoaling of the ocean mixed layer that remains 10 to 20 m too deep in the model as compared to the available observations.

4. Impact of the BL

[12] The sensitivity experiment is designed to quantify the impact of the BL on the SST. Figure 4a displays the April climatological SST difference (REF minus PERTURB). The solid line denotes the statistically significant area with a confidence level of 95% using a Student's T-test. Significant differences are observed from March to May. As expected, the presence of the BL favors the spring SST warming in the SEAS. REF experiment is warmer in the whole SEAS area with peak SST differences of 0.5°C in April, two months after the maximum of BL extension.

[13] The atmospheric response to this positive SST difference peaks in May (Figure 4). A statistically significant difference of the10 meter wind converges around 6°N over the gradient located at the south of SST difference. This brings additional moisture into the area and leads to a positive precipitation anomaly for the REF experiment. A maximum difference of 3 mm/day is observed. The time series of REF minus PERTURB precipitation (Figure 5b) show that the significant difference over the box (68°E–77°E; 3°N–10°N) occurs from mid-April to the end of May. It corresponds mainly to a temporal shift between REF and PERTURB precipitation (Figure 5a): PERURB monsoon onset (defined here as the period of massive increase of precipitations in the SEAS in spring) is delayed by 10 to 15 days. The modification of precipitation pattern is also associated in REF with larger evaporation (1 mm/day) and larger heat lost for the ocean (10W/m^2 larger latent heat flux and 15W/m^2 weaker solar heat flux) that acts against the SST warming in REF.

5. Conclusion

[14] For the first time, a complex and realistic coupled model has been used to quantify the impact of the salinity stratification on the climate variability in the SEAS. These first results support previous studies and suggest that the extent of the BL may be a useful predictor of the onset of the summer monsoon in the area with a two-month lead-time. In our simulation, the BL enhances the spring SST warming by 0.5°C in April, favors more precipitation in May (3 mm/day) and leads to an earlier (10 to 15 days) monsoon onset.

[15] Despite the good agreement between the coupled model simulations and the main climatic features in the region of interest, there are some biases that could affect our results. First, the model mixed layer is too deep in January–February. A comprehensive study of the heat budget in the mixed layer would be needed to understand the respective impact of multiple processes (penetrating solar heat flux,

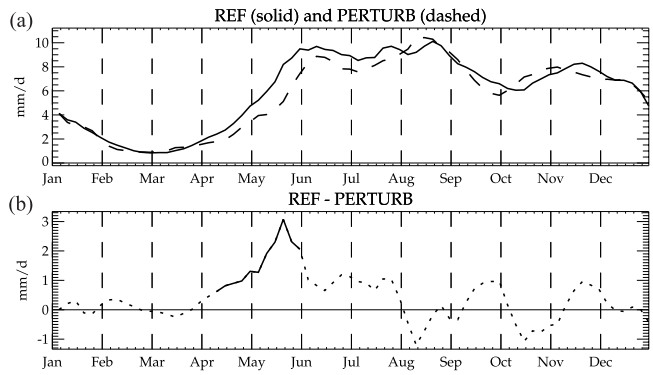

Figure 5. Time series averaged over (68°E–77°E, 3°N–10°N) of the 5 days climatological precipitation (mm/day). a: REF (PERTURB) in solid (dashed) line, b: difference (REF)-(PERTURB), significant values, 95% using a Student's T-test, in solid line.

inversion of the vertical gradient of temperature, thermal inertia of the mixed layer) on the robustness of our results regarding the model biases (stratification, heat fluxes). Second, we found that the main impact of the BL on the monsoon onset was concentrated over the ocean. While the BL effect might indeed be local, our atmospheric model shows some weakness to represent the mature phase on the Indian monsoon and its extent over the continent. It would be interesting to compare our results with other models results and test higher vertical and horizontal resolution of our atmospheric grid since it's one of the key factors to improve monsoon representation with ECHAM model [*Gualdi et al.*, 2003b].

[16] The next step of our research will focus on the possible links between the interannual variability of the BL and the rainfall in the SEAS. Suppressing the impact of salinity in the vertical mixing is a strong modification of the ocean physics. Would it be possible, as suggested by the present work, to use the extent of the BL as a useful predictor of the onset of the summer monsoon in the area with a two-month lead-time?

[17] **Acknowledgments.** This work would have been impossible without the technical support of our Japanese colleagues S. Shingu and H. Aiki and of numerous European collaborators involved into the SINTEX-F CGCM development: N. Grima, the MPI-ECHAM group, the LODYC-OPA and IPSL groups and CERFACS-OASIS group. All experiments have been performed using the Earth Simulator.

References

Bowman, K. P., A. B. Phillips, and G. R. North (2003), Comparison of TRMM rainfall retrievals with rain gauge data from the TAO/TRITON buoy array, *Geophys. Res. Lett.*, *30*(14), 1757, doi:10.1029/2003GL017552.

Bruce, J. G., D. R. Johnson, and J. C. Kindle (1994), Evidence for eddy formation in the eastern Arabian Sea during the northeast monsoon, *J. Geophys. Res.*, *99*, 7651–7664.

Bruce, J. G., J. C. Kindle, L. H. Kantha, J. L. Kerling, and J. F. Bailey (1998), Recent observations and modeling in the Arabian Sea Laccadive High region, *J. Geophys. Res.*, *103*, 7593–7600.

De Boyer Montegut, C., G. Madec, A. Fischer, A. Lazar, and D. Ludicone (2004), Mixed layer depth over the global ocean: An examination of profile data and a profile-based climatology, *J. Geophys. Res.*, *109*, C12003, doi:10.1029/2004JC002378.

Delcroix, T., A. Dessier, Y. Gouriou, and M. J. McPhaden (2005), Time and space scales for SSS in the tropical oceans, *Deep Sea Res., Part I*, in press.

Durand, F., S. R. Shetye, J. Vialard, D. Shankar, S. S. C. Shenoi, C. Ethe, and G. Madec (2004), Impact of temperature inversions on SST evolution in the south-eastern Arabian Sea during the pre-summer monsoon season, *Geophys. Res. Lett.*, *31*, L01305, doi:10.1029/2003GL018906.

Duvel, J. P., R. Roca, and J. Vialard (2004), Ocean mixed layer temperature variations induced by intraseasonal convective perturbations over the Indian Ocean, *J. Atmos. Sci.*, *61*, 1004–1023.

Gualdi, S., E. Guilyardi, A. Navarra, S. Masina, and P. Delecluse (2003a), The interannual variability in the tropical Indian Ocean as simulated by a CGCM, *Clim. Dyn.*, *20*, 567–582.

Gualdi, S., A. Navarra, E. Guilyardi, and P. Delecluse (2003b), Assessment of the tropical Indo-Pacific climate in the SINTEX CGCM, *Ann. Geophys.*, *46*, 1–26.

Guilyardi, E., P. Delecluse, S. Gualdi, and A. Navarra (2003), Mechanisms for ENSO phase change in a coupled GCM, *J. Clim.*, *16*, 1141–1158.

Kershaw, R. (1985), Onset of the south-west monsoon and sea surface temperature anomalies in the Arabian Sea, *Nature*, *315*, 561–563.

Krishnamurti, T. N., P. Ardanuy, Y. Ramanathan, and R. Pasch (1981), On the onset vortex of the summer monsoon, *Mon. Weather Rev.*, *109*, 344–363.

Lukas, R., and E. Lindstrom (1991), The mixed layer of the western equatorial Pacific Ocean, *J. Geophys. Res.*, *96*, 3343–3357.

Luo, J.-J., S. Masson, S. Behera, P. Delecluse, S. Gualdi, A. Navarra, and T. Yamagata (2003), South Pacific origin of the decadal ENSO-like variation as simulated by a coupled GCM, *Geophys. Res. Lett.*, *30*(24), 2250, doi:10.1029/2003GL018649.

Madec, G., P. Delecluse, M. Imbard, and C. Levy (1999), OPA 8.1 Ocean General Circulation Model reference manual, *Internal Rep. 11*, Inst. Pierre-Simon Laplace, Paris, France.

Nordeng, T. E. (1994), Extended versions of the convective parameterization scheme at ECMWF and their impact on the mean and transient activity of the model in the tropics, *Tech. Memo. 206*, Eur. Cent. for Medium-Range Weather Forecasts, Reading, UK.

Rao, R. R., and R. Shivakumar (1999), On the possible mechanism of the evolution of a mini-warm pool during the pre-summer monsoon season and the genesis of onset vortex in the south-eastern Arabian Sea, *Q. J. R. Meteorol. Soc.*, *125*, 787–809.

Rao, R. R., and R. Sivakumar (2003), Seasonal variability of sea surface salinity and salt budget of the mixed layer of the north Indian Ocean, *J. Geophys. Res.*, *108*(C1), 3009, doi:10.1029/2001JC000907.

Roeckner, E. (1996), The atmospheric general circulation model ECHAM-4: Model description and simulation of present-day climate, *Tech. Rep. 218*, 90 pp., Max-Planck-Inst. für Meteorol., Hamburg, Germany.

Sengupta, D., and M. Ravichandran (2001), Oscillations of Bay of Bengal sea surface temperature during the 1998 summer monsoon, *Geophys. Res. Lett.*, *28*, 2033–2036.

Sengupta, D., P. K. Ray, and G. S. Bhat (2002), Spring warming of the eastern Arabian Sea and Bay of Bengal from buoy data, *Geophys. Res. Lett.*, *29*(15), 1734, doi:10.1029/2002GL015340.

Shankar, D., and S. R. Shetye (1997), On the dynamics of the Lakshadweep high and low in the southeastern Arabian Sea, *J. Geophys. Res.*, *102*, 12,551–12,562.

Shenoi, S. S. C., D. Shankar, and S. R. Shetye (1999), On the sea surface temperature high in the Lakshadweep Sea before the onset of the south-west monsoon, *J. Geophys. Res.*, *104*, 15,703–15,712.

Shenoi, S. S. C., D. Shankar, and S. R. Shetye (2004), Remote forcing annihilates barrier layer in southeastern Arabian Sea, *Geophys. Res. Lett.*, *31*, L05307, doi:10.1029/2003GL019270.

Shetye, S. R., A. D. Gouveia, S. S. C. Shenoi, G. S. Michael, D. Sundar, A. M. Almeida, and K. Santanam (1991), The coastal current off western India during the northeast monsoon, *Deep Sea Res., Part A*, *38*, 1517–1529.

Sprintall, J., and M. Tomczak (1992), Evidence of the barrier layer in the surface layer of the tropics, *J. Geophys. Res.*, *97*, 7305–7316.

Tiedtke, M. (1989), A comprehensive mass flux scheme for cumulus parameterization in large-scale models, *Mon. Weather Rev.*, *117*, 1779–1800.

Valcke, S., L. Terray, and A. Piacentini (2000), *The OASIS Coupler User Guide Version 2.4*, 85 pp., Eur. Cent. for Res. and Adv. Training in Sci. Comput., Toulouse, France.

Vialard, J., and P. Delecluse (1998), An OGCM study for the TOGA decade, Part 1: Role of salinity in the physics of the western Pacific fresh pool, *J. Phys. Oceanogr.*, *28*, 1071–1088.

Vinayachandran, P. N. (2004), Summer cooling of the Arabian Sea during contrasting monsoon, *Geophys. Res. Lett.*, *31*, L13306, doi:10.1029/2004GL019961.

S. Behera, J.-J. Luo, S. Masson, and T. Yamagata, Frontier Research Center for Global Change (JAMSTEC), 3173-25 Showa-machi Kanazawa-ku, Yokohama-shi, Kanagawa 236-0001, Japan. (smasson@jamstec.go.jp)

P. Delecluse and E. Guilyardi, LSCE-IPSL, bat 709 CEA/Saclay, F-91191 Gif-sur-yvette, France.

F. Durand, LEGOS-IRD-UMR5566, 14 Avenue E. Belin, F-31400 Toulouse, France.

S. Gualdi and A. Navarra, National Institute of Geophysics and Volcanology, v. Donato Creti 12, I-40128 Bologna, Italy.

G. Madec and J. Vialard, LOCEAN-IPSL, Case 100, Université Pierre et Marie Curie, 4 Place Jussieu, F-75252 Paris, France.